

# Long-range triplet proximity effect in multiply connected ferromagnet-superconductor hybrids

A.V. Samokhvalov,<sup>1,2</sup> J.W.A. Robinson,<sup>3</sup> and A.I. Buzdin<sup>3,4,5</sup>

<sup>1</sup>*Institute for Physics of Microstructures, Russian Academy of Sciences, 603950 Nizhny Novgorod, GSP-105, Russia*

<sup>2</sup>*Lobachevsky State University of Nizhny Novgorod, Nizhny Novgorod 603950, Russia*

<sup>3</sup>*Department of Materials Science & Metallurgy, University of Cambridge, CB3 0FS Cambridge, United Kingdom*

<sup>4</sup>*University Bordeaux, LOMA UMR-CNRS 5798, F-33405 Talence Cedex, France*

<sup>5</sup>*Sechenov First Moscow State Medical University, Moscow, 119991, Russia*

Applying the linearized Usadel equations, we consider the nucleation of superconductivity in multiply connected mesoscopic superconductor/ferromagnet (S/F) hybrids such as a thin superconducting ring on a ferromagnet with a uniform in-plane magnetization  $M$  and a spin-active S/F interface. We demonstrate that the exchange field in F provokes a switching between superconducting states with different vorticities which may increase the critical temperature ( $T_c$ ) of the superconductor in a magnetic field. We study the interplay between oscillations in  $T_c$  due to the Little-Parks effect and oscillations in  $T_c$  induced by the exchange field. Furthermore, we analyse the influence of long-range spin-triplet correlations on the switching between different vorticities.

PACS numbers: 74.45.+c, 74.25.Dw, 74.78.Na

## I. INTRODUCTION

In hybrid systems containing superconducting and ferromagnetic metals (see reviews<sup>1-6</sup>), long-range correlations are induced in the ferromagnets<sup>7-14</sup> related to odd-frequency superconductivity<sup>15</sup> and spin-polarized triplet Cooper pairs<sup>16,17</sup>. Such long-range spin-triplet pairs are not destroyed by a ferromagnetic exchange field and can penetrate a ferromagnet over long distances exceeding a singlet pair coherence length. The reduction of a Co nanowire's resistance in contact with a superconductor observed in<sup>7,18</sup> as the temperature is decreased below the superconducting transition, demonstrated evidence for a long-range proximity effect. Evidence for electron pair conversion from spin-singlet to spin-triplet has recently been demonstrated via observations of long-ranged supercurrents in S/F/S Josephson junctions with magnetically inhomogeneous S/F interfaces<sup>11-14,19-23</sup>, transition temperature measurements of S/F1/F2 spin valves<sup>24-29</sup>, density of states measurements on S/F systems<sup>30-37</sup> and ferromagnetic resonance<sup>38,39</sup>. The optimal condition for pair conversion in a dirty ferromagnet is realized when the exchange field  $h$  is inhomogeneous on scale of the coherence length  $\xi_f = \sqrt{\hbar D_f/h}$  in the F<sup>40</sup>, where  $D_f$  is the electron diffusion constant. Under appropriate conditions, odd-frequency spin-triplet correlations manifest as an intrinsic paramagnetic Meissner state<sup>41-43</sup>. The existence of an anomalous Meissner response has been observed via a depth-resolved measurements of the local magnetic fields in Au/Ho/Nb using low-energy muons<sup>44</sup>.

Long-range proximity effect have mainly focused on mesoscopic ferromagnetic wires attached to a superconductor or layered (diffusive) S/F structures. Here we propose using multiply connected hybrid S/F structures such as a thin narrow superconducting ring on a ferromagnetic plate (see Fig. 1(a)) to study proximity-induced long-range triplet correlations. A distinguishing feature of

multiply connected S/F hybrids with the proximity effect is the generation of a vortex state with a nonzero orbital angular momentum  $L$  (vorticity) even in the absence of an external magnetic field<sup>45</sup>. The damped oscillations of the amplitude of singlet superconducting correlations in a ferromagnet in the direction perpendicular to the S/F interface<sup>46-48</sup> generates the additional phase modulation of superconducting order parameter  $\Delta \sim \exp(iL\theta)$  on azimuthal angle  $\theta$  and may induce spontaneous supercurrents. The angular momentum  $L$  of the pair wave function determines the vorticity of the state. The interplay between orbital<sup>49</sup> and the exchange<sup>50</sup> effects may result in a switching between the states with different vorticities  $L$ , as the ring radius  $R_1$  increases. Transitions between states with different  $L$  result in a nonmonotonic dependence of the critical temperature  $T_c$  on  $R_1$  and  $h$ .

The Little-Parks (LP) effect (the periodic oscillations of the critical temperature  $T_c$  of a hollow superconducting cylinder in an applied magnetic field  $H$ <sup>51,52</sup>) is an extremely sensitive experimental tool for studying interference phenomena in multiply connected superconducting systems. The orbital effect results in switching between states with different vorticity  $L$  and manifests itself in oscillations of the phase-transition line  $T_c(H)$ . The interplay between  $T_c$  oscillations due to LP effect and oscillations due to  $h$  in multiply connected S/F hybrids with a uniform magnetization was shown to be accompanied by breaking of the strict periodicity of  $T_c(H)$  oscillations and shifts in  $T_c$  maximum to finite  $H$ <sup>53</sup>. Similar results were obtained later in<sup>54,55</sup> for the case of a spiral exchange field distribution in a ferromagnet. Note, however, that in the case of a magnetic spiral, equal-spin triplet pairs do not arise, and long-range proximity induced superconductivity is absent<sup>6,56</sup>.

The aim of our paper is to examine the long-range proximity effect on switching between vortex states in multiply connected S/F hybrids. We expect that the superconducting ground state in such a geometry should be

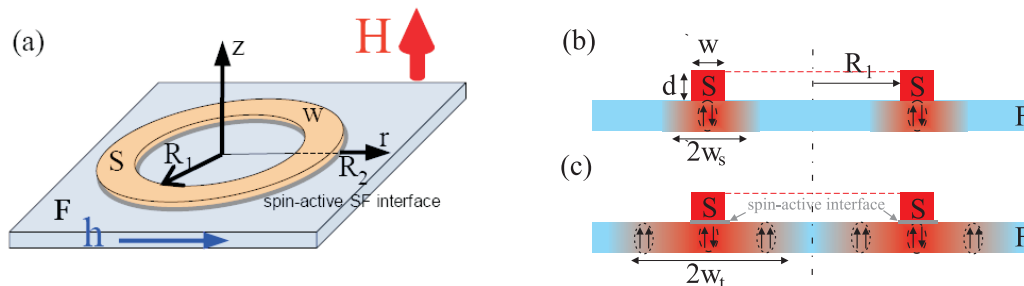


FIG. 1: (Color online) (a) A superconducting ring (S) on the surface of a ferromagnetic plate (F) with a uniform exchange field  $\mathbf{h}$  and a spin-active S/F interface. Here  $R_1$  ( $R_2$ ) and  $w = R_2 - R_1$  are the inner (outer) radius and the width of the S ring,  $(r, \theta, z)$  is the cylindrical coordinate system. The external magnetic field  $\mathbf{H}$  is applied along the  $z$  axis. (b) Short-range proximity-induced superconductivity in a F metal. (c) Long-range proximity induced superconductivity in a F metal due to the presence of a spin-active S/F interface. Arrows indicate the spin structure of pair correlations in F.

strongly influenced by the presence of equal-spin triplet pairs in F. We focus on the behavior of  $T_c$  for superconducting states with different vorticities, and study the influence of the equal-spin triplet components on LP oscillations. We start from a qualitative discussion of the long-range proximity effect on the LP oscillations in a superconducting ring lying on a thin F (see Fig. 1(a)). We assume that  $R_1 \gg \xi_f \gg w$ . In the absence of equal-spin triplet superconducting correlations, proximity-induced superconductivity in F occupies the region  $w_s \approx w + 2\xi_f \ll R_1$  under the S ring (Fig. 1(b)). As a result, the period of the LP oscillations  $\Delta H^{(s)}$  is modified due to the small increase of the ring width  $w_s \gtrsim w$  where superconductivity coexists<sup>57</sup>, i.e.,

$$\Delta H^{(s)} \sim \frac{\Phi_0}{\pi R_1^2 [1 + (w_s/R_1)^2]},$$

and a slow modulation of the amplitude of the LP oscillations takes place<sup>53</sup>. Here  $\Phi_0 = \pi \hbar c / |e|$  is the magnetic flux quantum.

Long-range equal-spin triplet pairs exist over a distance of the order the thermal length  $\xi_n = \sqrt{\hbar D_f / 2\pi T_{cs}} \gg \xi_f$ , and proximity-induced superconductivity in F occupies the region  $w_t \approx \xi_n \gtrsim R_1$  (Fig. 1(c)). Here,  $T_{cs}$  is the transition temperature of the superconductor in the absence of a proximity effect, i.e.  $T_c$  of S without F and an applied magnetic field. In this case the spin-triplet pairs dominate a considerable part of the S/F structure, as shown in Fig. 1c. It has recently been demonstrated that the spin-triplet odd-frequency superconducting correlations emerging in layered S/F systems favor the formation of the in-plane FFLO phase with the gap potential modulated along the S/F interface<sup>43,58</sup>. A hallmark of in-plane FFLO instability is a vanishing of the London magnetic field penetration depth  $\lambda(\mathbf{r})$  averaged over the structure volume. In multiply connected S/F structures the in-plane FFLO instability is expected to provoke a modification of  $T_c(H)$  which correspond to the switching between modes with the different vorticity  $L$ . This effect should be especially important if  $R_1 \gg \xi_f$ , because of the mechanism of vor-

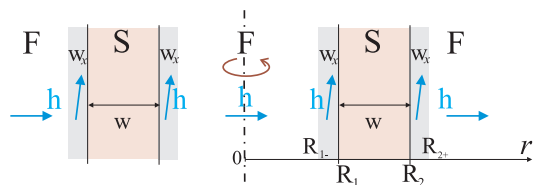


FIG. 2: (Color online) Cross section of the model cylindrical structure under consideration. The blue arrows show the direction of the exchange field  $\mathbf{h}$  in the ferromagnet (F).

text states switching (caused by the oscillatory behavior spin-singlet pair wave function in a ferromagnet<sup>45</sup>) in this case is suppressed. The experimental observation of the unusual behavior of the Little-Parks oscillations predicted here would provide direct evidence of spin-polarized triplet Cooper pairs.

The paper is organized as follows. In Sec. II we describe the model of a multiply connected S/F system and briefly discuss basic equations. In Sec. III we proceed with the analytic calculations of  $T_c$  for different vortex states. In Sec. IV we study the proximity induced switching between different vortex states in the absence of an applied magnetic field. We show that transitions between states with different vorticity are accompanied by jumps of effective magnetic field penetration depth. Moreover we analyse the influence of the long-range spin-triplet correlations on the realisation of the states with higher vorticities. The interplay between the oscillations of  $T_c$  due to the LP effect and oscillations due to the  $h$  is analyzed in Sec. V. We summarize our results in Sec. VI.

## II. MODEL AND BASIC EQUATIONS

The planar F/S system under consideration (Fig. 1(a)) was shown to be qualitatively similar to a hollow superconducting cylinder surrounded by a ferromagnetic metal<sup>45</sup>. Hereafter, we consider a model S/F system consisting of a thin-walled hollow S cylinder embedded in a

ferromagnetic metal. The cross section of the model S/F structure is shown in Fig. 2. The surrounding F metal has a uniform exchange field  $\mathbf{h}$  and spin-active S/F interfaces. A good electrical contact between the F and S metals is assumed to provide a strong proximity effect. The S and F metals have diffusion coefficients  $D_s$  and  $D_f$ , respectively, and satisfy the dirty limit where  $T_{cs}\tau/\hbar \ll 1$  and  $h\tau/\hbar \ll 1$ . Here,  $\tau = l/v_F$  is the electron elastic scattering time with the electron mean free path  $l$ . To observe a pronounced influence of the proximity effect on  $T_c$ , the thickness of the S shell  $w = R_2 - R_1$  must be smaller than the superconducting coherence length  $\xi_s = \sqrt{\hbar D_s/2\pi T_{cs}}$ . The exchange field  $\mathbf{h}$  acting on the spin of the conduction electrons is assumed to have step-like profile

$$\mathbf{h}(r) = \begin{cases} h\tilde{z}, & r \leq R_1 - w_x \\ h\tilde{z}, & r \geq R_2 + w_x \\ h\tilde{z} + h_x(r)\tilde{x}, & R_1 - w_x \leq r \leq R_1 \\ 0, & R_2 \leq r \leq R_2 + w_x \\ 0, & R_1 < r \leq R_2, \end{cases} \quad (1)$$

where  $\tilde{x}, \tilde{z}$  are the axes for spin quantization. We neglect reduction of the magnetization in the ferromagnet and magnetization leakage into the superconductor due to the magnetic proximity effect<sup>61–63</sup>. The spin-active interface between S and F is described by the rotation of the exchange field  $\mathbf{h}$  in thin cylindrical layers  $R_1 - w_x \leq r \leq R_1$  and  $R_2 \leq r \leq R_2 + w_x$  near F/S interfaces provided  $w_x \ll \xi_f, R_1$  but the product  $\int dr h_x(r)/w_x h$  is of the order unity<sup>40</sup>.

Our calculations of the second-order superconducting phase transition temperature  $T_c$  are based on solutions of the linearized Usadel equations<sup>64</sup>. At  $T \sim T_c$ , the normal Green function  $g$  coincides with the value in the normal state ( $g \simeq -i \text{sgn} \omega_n$ ), and the linearized Usadel equations for anomalous quasiclassical Green's function<sup>6,65,66</sup>

$$\hat{f}_{s,f} = f_{s,f}^s + \mathbf{f}_{s,f}^t \hat{\sigma}, \quad \mathbf{f}_{s,f}^t = f_{s,f}^z \mathbf{z}_0 + f_{s,f}^x \mathbf{x}_0 \quad (2)$$

take the form (see reviews<sup>1,3,67</sup> for details):

$$-\frac{\hbar D_{s,f}}{2} \left( \nabla - \frac{2ie}{\hbar c} \mathbf{A} \right)^2 f_{s,f}^s + |\omega_n| f_{s,f}^s + i \text{sgn} \omega_n (\mathbf{h} \mathbf{f}_{s,f}^t) = \Delta, \quad (3)$$

$$-\frac{\hbar D_{s,f}}{2} \left( \nabla - \frac{2ie}{\hbar c} \mathbf{A} \right)^2 \mathbf{f}_{s,f}^t + |\omega_n| \mathbf{f}_{s,f}^t + i \text{sgn} \omega_n \mathbf{h} f_{s,f}^s = 0. \quad (4)$$

Here, where  $f_{s,f}^s(\mathbf{r}, \omega_n)$  ( $\mathbf{f}_{s,f}^t(\mathbf{r}, \omega_n)$ ) is the singlet (triplet) part of the Green's function (2) in the superconductor and ferromagnet,  $\omega_n = (2n+1)\pi T_c$  is the Matsubara frequency at the temperature  $T_c$ ,  $\Delta = \Delta_s$  is the singlet pairing potential inside superconductor ( $\Delta = 0$  in ferromagnet), and  $\mathbf{A}$  is the vector potential of the external magnetic field  $\mathbf{H} = \text{rot} \mathbf{A} = H \mathbf{z}_0$ . We have neglected the effect of the ferromagnet magnetization  $\mathbf{M}$  because of the additional magnetic flux enclosed by the

S shell  $\Phi_M \approx 4\pi^2 R_1^2 M$  is assumed to be small in comparison with the magnetic flux quantum  $\Phi_0 = \pi \hbar c / |e|$  for typical parameters of S/F hybrids<sup>53</sup>. The Usadel equations (3),(4) must be supplemented with the Kupriyanov-Lukichev boundary conditions<sup>68</sup> for all components of the Green function (2) at the S/F interfaces  $r = R_1$  and  $r = R_2$ :

$$\sigma_s \partial_r \hat{f}_s = \sigma_f \partial_r \hat{f}_f, \quad \hat{f}_s = \hat{f}_f + \gamma_b \xi_n \partial_r \hat{f}_f. \quad (5)$$

Here  $\sigma_f$  and  $\sigma_s$  are the normal-state conductivities of the F and S metals,  $\gamma_b$  is related to the transparency of the S/F interface and is determined by the boundary resistance per unit area  $R_b$ :  $\gamma_b \xi_s = R_b \sigma_f$ .

The  $T_c$  is determined by the self-consistency equation for the singlet gap function  $\Delta_s$ :

$$\Delta_s(\mathbf{r}) \ln \frac{T_c}{T_{cs}} + \pi T_c \sum_{\omega_n} \left( \frac{\Delta_s(\mathbf{r})}{\omega_n} - f_s^s(\mathbf{r}, \omega_n) \right) = 0. \quad (6)$$

For simplicity of  $T_c$  calculations, we assume  $h \gg T_{cs}$  and neglect proximity suppression caused by a finite S/F interface resistance, i.e., we take  $\gamma_b = 0$  in (5). In this regime,  $\hat{f}_s = \hat{f}_f$  at the S/F interface.

Choosing the cylindrical coordinate system  $(r, \theta, z)$  and the gauge  $\mathbf{A} = (0, A_\theta, 0)$ ,  $A_\theta = rH/2$  we consider homogeneous along  $z$  solutions of the equations (3),(4), characterized by a certain angular momentum  $L$ , referred further as vorticity

$$\Delta_s(\mathbf{r}) = \Delta_L(r) e^{iL\theta}, \quad f^{s,z,x}(\mathbf{r}, \omega_n) = f_L^{s,z,x}(r, \omega_n) e^{iL\theta}. \quad (7)$$

The vorticity parameter  $L$  in (7) coincides with the angular momentum of the Cooper pair wave function.

According to Eqs. (3),(4),(6) there is a symmetry  $f^s(r, -\omega_n) = f^s(r, \omega_n)$  and  $f^{z,x}(r, -\omega_n) = -f^{z,x}(r, \omega_n)$ , so that we can treat only positive  $\omega_n$  values. The Usadel equations (3) and (4) can be written in the form

$$-\frac{\hbar D}{2} \hat{Q}_L f_L^s + \omega_n f_L^s + \imath h f_L^z + \imath h_x f_L^x = \Delta_L, \quad (8)$$

$$-\frac{\hbar D}{2} \hat{Q}_L f_L^x + \omega_n f_L^x + \imath h_x f_L^s = 0, \quad (9)$$

$$-\frac{\hbar D}{2} \hat{Q}_L f_L^z + \omega_n f_L^z + \imath h f_L^s = 0, \quad (10)$$

$$\hat{Q}_L = \frac{1}{r} \frac{d}{dr} \left( r \frac{d}{dr} \right) - \left( \frac{L - \phi_r}{r} \right)^2$$

where  $D = D_{s,f}$  is the diffusion coefficient in S and F, respectively,  $\phi_r = \pi r^2 H / \Phi_0$  is a dimensionless flux of the external magnetic field  $H$  threading the circle of certain radius  $r$ . As follows from Eqs. (8),(9),(10), if the gap potential  $\Delta_L$  is real, the components  $f_L^s$  of the anomalous Green's function are also real, while the components  $f_L^x$  and  $f_L^z$  are imaginary. Then it is convenient to introduce the complex function<sup>69</sup>

$$F(r) = f_L^s + \imath f_L^z \quad (11)$$

and the real function

$$P(r) = -i f_L^x, \quad (12)$$

so that

$$f_L^s = \text{Re}[F], \quad f_L^z = i \text{Im}[F], \quad \text{and} \quad f_L^x = i P. \quad (13)$$

These functions satisfy the equations

$$-\frac{\hbar D}{2} \hat{Q}_L F + (\omega_n + i h) F - h_x P = \Delta_L, \quad (14)$$

$$-\frac{\hbar D}{2} \hat{Q}_L P + \omega_n P + h_x \text{Re}[F] = 0. \quad (15)$$

The boundary conditions for  $F$  and  $P$  follow directly from the conditions (5) for  $\hat{f}$  components.

### III. $T_c$ OF VORTEX STATES

We proceed with  $T_c$  calculations for different vortex states (7).

#### A. Solution inside the F core: ( $r \leq R_1$ )

The solution of Eqs. (14),(15) in the F cylinder  $r \leq R_1 - w_x$  with uniform exchange field  $\mathbf{h} = h \mathbf{z}_0$  can be expressed via the confluent hypergeometric function of the first kind (Kummer's function)  $K(a, b, z)$ <sup>70</sup>

$$F_{f1}(r) = C_1 e^{-\phi_r/2} \phi_r^{L/2} K(a_{Ln}, b_L, \phi_r), \quad (16)$$

$$P_{f1}(r) = C_2 e^{-\phi_r/2} \phi_r^{L/2} K(a_{Ln}^r, b_L, \phi_r), \quad (17)$$

where

$$a_{Ln} = \frac{|L| - L + 1}{2} + \frac{(\omega_n + i h) R_1^2}{2 \hbar D_f \phi_1},$$

$$a_{Ln}^r = \text{Re}[a_{Ln}], \quad b_L = |L| + 1$$

and  $\phi_1 = \pi R_1^2 H / \Phi_0$  is a dimensionless flux of the external magnetic field  $\mathbf{H}$  threading the circle of the radius  $R_1$ . To proceed further with tractable formulas, we take into account that the spin-active layer near the interface  $r = R_1$  is thin ( $w_x \ll \xi_f, R_1$ ). After averaging Eqs. (16),(17) over the thickness of thin  $w_x \rightarrow 0$  layer one can receive the following relations between the values of the functions  $F_{f1}, P_{f1}$  and their derivatives  $\partial_r F_{f1}, \partial_r P_{f1}$  at the S/F interface  $r = R_1$ :

$$\frac{dF_{f1}}{dr} = \frac{\kappa_{Ln}}{R_1} F_{f1} - \frac{2\delta}{\xi_f} P_{f1}, \quad (18)$$

$$\frac{dP_{f1}}{dr} = \frac{\mu_{Ln}}{R_1} P_{f1} + \frac{2\delta}{\xi_f} \text{Re}[F_{f1}], \quad (19)$$

where  $\delta$ , characterizing the spin-activity of the S/F interface, is determined by

$$\delta = \frac{\xi_f}{\hbar D_f} \int_{R_1 - w_x}^{R_1} h_x(r) dr, \quad (20)$$

and

$$\begin{aligned} \kappa_{Ln} &\equiv \kappa_{Ln}(\phi_1) = |L| - \phi_1 \\ &+ 2\phi_1 \frac{a_{Ln} K(a_{Ln} + 1, b_L + 1, \phi_1)}{b_L K(a_{Ln}, b_L, \phi_1)}, \end{aligned} \quad (21)$$

$$\begin{aligned} \mu_{Ln} &\equiv \mu_{Ln}(\phi_1) = |L| - \phi_1 \\ &+ 2\phi_1 \frac{a_{Ln}^r K(a_{Ln}^r + 1, b_L + 1, \phi_1)}{b_L K(a_{Ln}^r, b_L, \phi_1)}. \end{aligned} \quad (22)$$

#### B. Solution in outer ferromagnet: ( $r \geq R_2$ )

The solution of Eqs. (14),(15) in ferromagnet with a cylindrical cavity of radius  $r = R_2$  can be expressed via the confluent hypergeometric function of the second kind  $U(a, b, z)$ <sup>70</sup>

$$F_{f2}(r) = \tilde{C}_1 e^{-\phi_r/2} \phi_r^{L/2} U(a_{Ln}, b_L, \phi_r), \quad (23)$$

$$P_{f2}(r) = \tilde{C}_2 e^{-\phi_r/2} \phi_r^{L/2} U(a_{Ln}^r, b_L, \phi_r). \quad (24)$$

As before the spin-active layer near the S/F interfaces ( $r = R_2$ ) is assumed to be thin and described by  $\delta$  (20). The relations between the values of the functions  $F_{f2}, P_{f2}$  and their derivatives  $\partial_r F_{f2}, \partial_r P_{f2}$  at the S/F interfaces  $r = R_2$  are as follows:

$$\frac{dF_{f2}}{dr} = \frac{\tilde{\kappa}_{Ln}}{R_2} F_{f2} + \frac{2\delta}{\xi_f} P_{f2}, \quad (25)$$

$$\frac{dP_{f2}}{dr} = \frac{\tilde{\mu}_{Ln}}{R_2} P_{f2} - \frac{2\delta}{\xi_f} \text{Re}[F_{f2}], \quad (26)$$

where

$$\begin{aligned} \tilde{\kappa}_{Ln} &\equiv \tilde{\kappa}_{Ln}(\phi_2) = |L| - \phi_2 \\ &- 2\phi_2 \frac{a_{Ln} U(a_{Ln} + 1, b_L + 1, \phi_2)}{U(a_{Ln}, b_L, \phi_2)}, \end{aligned} \quad (27)$$

$$\begin{aligned} \tilde{\mu}_{Ln} &\equiv \tilde{\mu}_{Ln}(\phi_2) = |L| - \phi_2 \\ &- 2\phi_2 \frac{a_{Ln}^r U(a_{Ln}^r + 1, b_L + 1, \phi_2)}{U(a_{Ln}^r, b_L, \phi_2)}. \end{aligned} \quad (28)$$

and  $\phi_2 = \pi R_2^2 H / \Phi_0$  is the flux of the external magnetic field enclosed in the cavity of radius  $R_2$  in units of  $\Phi_0$ .

#### C. Solution in thin superconducting shell: ( $R_1 \leq r \leq R_2$ )

In absence of an exchange field, equations (14) and (15) in the superconducting region  $R_1 \leq r \leq R_2$  take the form

$$-\frac{\hbar D_s}{2} \hat{Q}_L F_s + \omega_n F_s = \Delta_L, \quad (29)$$

$$-\frac{\hbar D_s}{2} \hat{Q}_L P_s + \omega_n P_s = 0. \quad (30)$$

Assuming that variations of  $F_s(r), P_s(r)$  and  $\Delta_L(r)$  in the thin S shell are small for  $w \lesssim \xi_s, R_1$ , we can average Eqs. (29) and (30) over the thickness, using the

Kupriyanov-Lukichev boundary conditions (5) and relations (18),(19) (25),(26) to integrate the terms  $\partial_r(r \partial_r F_s)$  and  $\partial_r(r \partial_r P_s)$ . Finally, we obtain the following equations

$$(\bar{\Omega}_n + \nu_{Ln}) F_s - \epsilon P_s = \bar{\Delta}_L, \quad (31)$$

$$(\bar{\Omega}_n + \eta_{Ln}) P_s + \epsilon Re[F_s] = 0, \quad (32)$$

where  $\bar{\Omega}_n = \Omega_n/T_{cs}$ ,  $\bar{\Delta}_L = \Delta_L/T_{cs}$ ,

$$\Omega_n = \omega_n + \frac{D_s (L - \phi_1)^2}{2 R_1^2}, \quad \beta = \frac{\pi \xi_s^2 \sigma_f / \sigma_s}{w R_1},$$

$$\nu_{Ln} = \nu_{Ln}^r + i \nu_{Ln}^i = \beta (\kappa_{Ln} - \tilde{\kappa}_{Ln}),$$

$$\eta_{Ln} = \beta (\mu_{Ln} - \tilde{\mu}_{Ln}), \quad \epsilon = 2\beta\delta (R_1 + R_2) / \xi_f^2.$$

Solution of the algebraic system (31),(32) determines the amplitudes  $\bar{f}_L^s, \bar{f}_L^z, \bar{f}_L^x$  of the anomalous Green's functions (5) in superconductor for the orbital mode  $L$ :

$$\bar{f}_L^s = \frac{\bar{\Delta}_L (\bar{\Omega}_n + \nu_{Ln}^r)}{|\bar{\Omega}_n + \nu_{Ln}|^2 + \epsilon^2 (\bar{\Omega}_n + \nu_{Ln}^r) / (\bar{\Omega}_n + \eta_{Ln})}, \quad (33)$$

$$\bar{f}_L^z = \frac{-i \nu_{Ln}^i}{\bar{\Omega}_n + \nu_{Ln}^r} \bar{f}_L^s, \quad \bar{f}_L^x = \frac{-i \epsilon}{\bar{\Omega}_n + \eta_{Ln}} \bar{f}_L^s. \quad (34)$$

Substituting solution (33) into Eq. (6) one obtains a self-consistency equation for the critical temperature  $T_L$  of the state with a vorticity  $L$ :

$$\ln \frac{T_L}{T_{cs}} + \pi T_L \sum_{\omega_n} \left( \frac{1}{\omega_n} - \frac{\bar{f}_L^s}{\Delta_L} \right) = 0. \quad (35)$$

As usual, the critical temperature  $T_c$  of a superconductivity nucleation in the S/F hybrid is determined by the maximal value  $T_L$ :

$$T_c = \max\{T_L\}. \quad (36)$$

#### IV. PROXIMITY INDUCED VORTEX STATES

We start our analysis for the case of zero external magnetic field focusing on the effect of the S/F interface spin-activity and long-range triplet generation on the phase transition line  $T_c(R_f)$ . The solution of Eqs. (14),(15) for  $H = 0$  in the ferromagnet can be expressed via the modified Bessel functions  $I_L(\zeta)$  and  $K_L(\zeta)$  of the order  $L$ :

$$F_{f1}(r) = \sum_{\omega_n} \bar{F}_L(\omega_n) \frac{I_L(k_n r)}{I_L(k_n R_1)}, \quad r \leq R_1 - w_x, \quad (37)$$

$$P_{f1}(r) = \sum_{\omega_n} \bar{P}_L(\omega_n) \frac{I_L(q_n r)}{I_L(q_n R_1)},$$

$$F_{f2}(r) = \sum_{\omega_n} \bar{F}_L(\omega_n) \frac{K_L(k_n r)}{K_L(k_n R_2)}, \quad r \geq R_2 + w_x, \quad (38)$$

$$P_{f1}(r) = \sum_{\omega_n} \bar{P}_L(\omega_n) \frac{K_L(q_n r)}{K_L(q_n R_2)},$$

where  $\bar{F}_L = \bar{f}_L^s + \bar{f}_L^z$ ,  $\bar{P}_L = -i \bar{f}_L^x$ ,  $q_n = \xi_n^{-1} \sqrt{T_c(2n+1)/T_{cs}}$ ,  $k_n^2 = q_n^2 + 2i/\xi_f^2$ . Taking into account the solutions (37),(38) we obtain the following simplified expressions for the parameters  $\kappa_{Ln}$  (21),  $\mu_{Ln}$  (22),  $\tilde{\kappa}_{Ln}$  (27),  $\tilde{\mu}_{Ln}$  (28):

$$\begin{aligned} \kappa_{Ln} &= |L| + \frac{(k_n R_1) I_{L+1}(k_n R_1)}{I_L(k_n R_1)}, \\ \mu_{Ln} &= |L| + \frac{(q_n R_1) I_{L+1}(q_n R_1)}{I_L(q_n R_1)}, \\ \tilde{\kappa}_{Ln} &= |L| - \frac{(k_n R_2) K_{L+1}(k_n R_2)}{K_L(k_n R_2)}, \\ \tilde{\mu}_{Ln} &= |L| - \frac{(q_n R_2) K_{L+1}(q_n R_2)}{K_L(q_n R_2)}, \end{aligned}$$

which have to be used in expressions to calculate the critical temperature  $T_L$  of the proximity induced state with a vorticity  $L$ . Note, that the states with angular momenta  $\pm L$  are degenerated for  $H = 0$  and have the same critical temperature  $T_{-L} = T_L$ .

In Fig. 3 we show example dependencies of  $T_c$  versus  $R_1$  for different values of  $\delta$  characterizing the spin-activity of the S/F interface. We see that generation of long triplet correlations in F metal produces an additional depairing effect which results in a overall decrease in  $T_c$  for arbitrary  $L$ . At the same time, the destructive action of long-range proximity effect reduces the region of  $R_1$  where the vortex free state  $L = 0$  dominates, and provokes the appearance of the states with nonzero orbital momentum  $L \neq 0$ . Note that for strong enough spin-flip scattering at the S/F interface, the  $T_c(R_1)$  phase boundary exhibits quasiperiodic oscillations as function of the ring radius in the region  $R_1 \gg \xi_f$  (see Fig. 3(c),(d)). In this case the influence of damped-oscillatory behavior of the singlet  $f_L^s$  and the short triplet  $f_L^z$  components of superconducting correlations is weak and cannot provoke switching between the superconducting states with different vorticities.

In Fig. 4 we have plotted the spatial dependence of  $f_L^s$  and  $f_L^{z,x}$  components of the quasiclassical Green's function  $\hat{f}$  (2) for two different radii of the ring. One can see that  $f_L^s$  and short-range triplet  $f_L^z$  decay and oscillate on the scale  $\xi_f$  while the long-range triplet component  $f_L^x$  decays to zero slowly. As a result, the triplet component  $f_L^x$  dominates over a considerable part of the S/F structure. Note that recently it was demonstrated that the spin-triplet superconducting correlations emerging in S/F system favors the formation of the in-plane FFLO phase with the gap potential modulated along the S/F interface<sup>43</sup>. In our case this FFLO-like phase is revealed by the formation of the high vorticity states at large  $R_1$  radius - see Fig. 3(c),(d). A hallmark of in-plane FFLO instability is vanishing of the London magnetic field penetration depth  $\lambda(\mathbf{r})$  averaged over the structure volume.

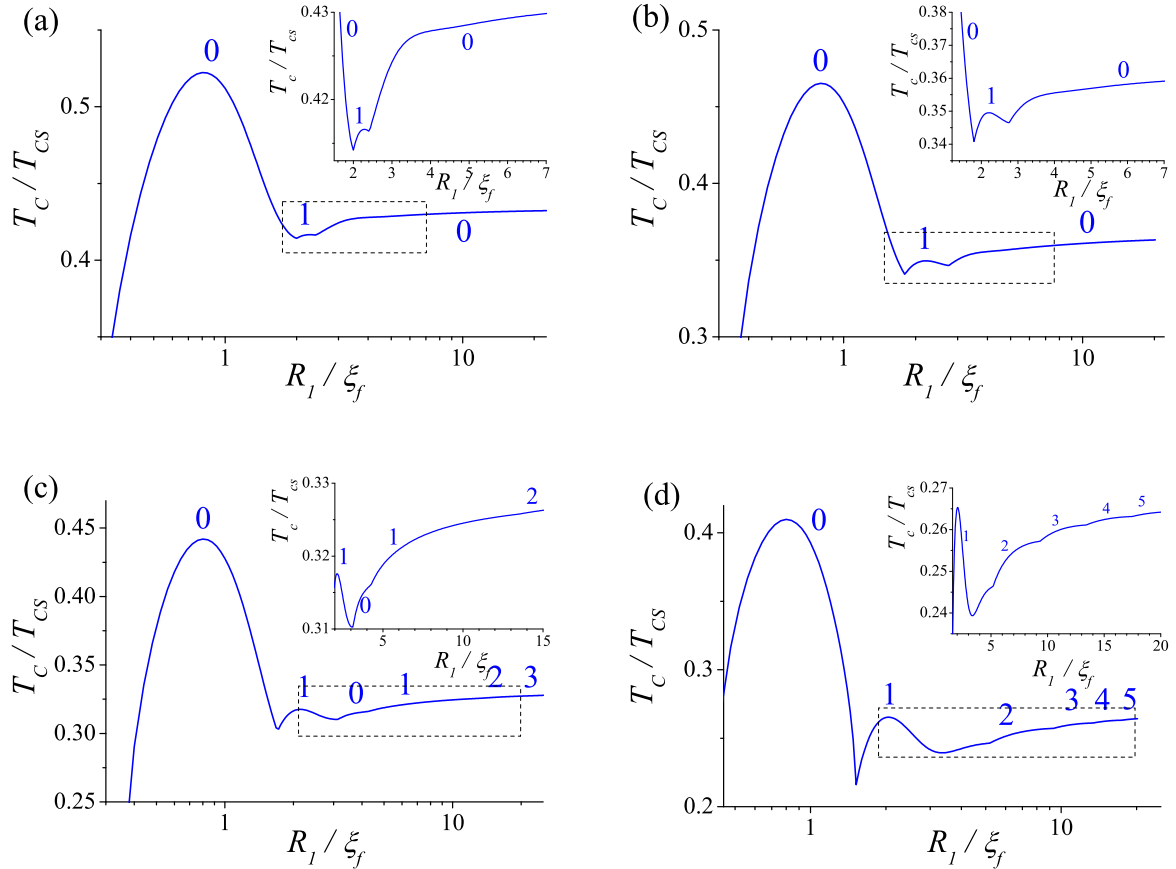


FIG. 3: (Color online) Typical dependences of  $T_c$  on the internal radius  $R_1$  of the S ring in zero applied field ( $H = 0$ ) for different values of  $\delta = \delta_1 + \delta_2$  characterizing the spin-activity of the S/F interface: (a)  $\delta = 0$ ; (b)  $\delta = 0.25$ ; (c)  $\delta = 0.3$ ; (d)  $\delta = 0.35$ . The numbers near the curves denote the corresponding vorticity  $L$ . The insets show the zoom in the part of the curves in the rectangles. Here we choose  $w = 0.6 \xi_s$ ;  $\xi_s/\xi_f = 0.1$ ;  $\xi_n/\xi_f = 5$ ;  $\sigma_f/\sigma_s = 0.5$ .

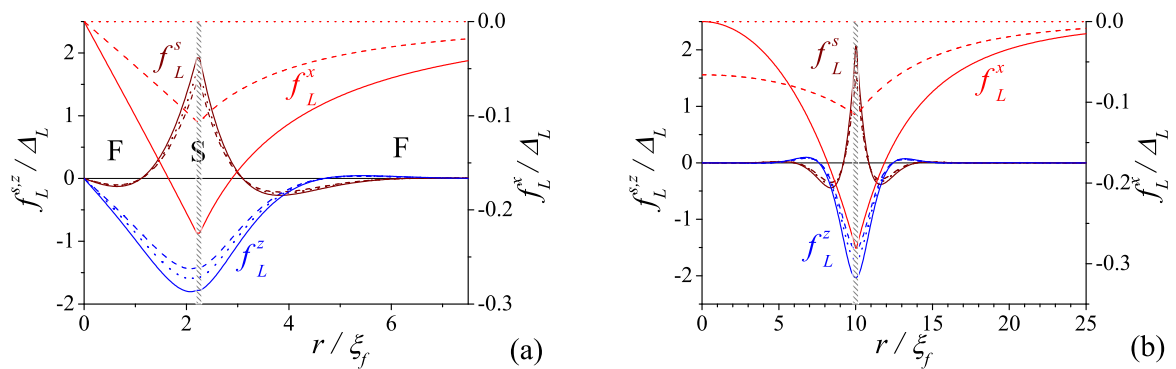


FIG. 4: (Color online) Spatial dependence of the components  $f_L^{s,z,x}$  (vorticity  $L = 1$ ) of the Green function  $\hat{f}$  (2) in zero applied field ( $H = 0$ ) for different values of the the ring radius: (a)  $R_1 = 2.2 \xi_f$ ; (b)  $R_1 = 10.0 \xi_f$  and for different values of the parameters  $\delta$  characterizing a spin-activity of the S/F interface:  $\delta = 0$  (dotted line);  $\delta = 0.25$  (dashed line);  $\delta = 0.35$  (solid line). The other parameters are the same as in Fig. 3.

#### A. Effective magnetic field penetration depth

To calculate the London penetration depth  $\lambda(\mathbf{r})$  that appears in relation

$$\mathbf{j} = \frac{c}{4\pi\lambda^2} \left( \frac{\hbar c}{2e} \nabla\phi - \mathbf{A} \right), \quad (39)$$

between screening current density  $\mathbf{j}$  and vector potential  $\mathbf{A}$ , we can use the expression for the  $k$  projection of the

supercurrent in terms of quasi-classical Usadel functions  $\hat{f}(\mathbf{r}, \omega_n)$  defined by the parametrization (2)<sup>6</sup>

$$j_{s,f}^k = \pi T_c \frac{\sigma_{s,f}}{e} \sum_{\omega_n} \text{Im} \left[ (f_{s,f}^s)^* \tilde{\nabla}_k f_{s,f}^s - (\mathbf{f}_{s,f}^t)^* \tilde{\nabla}_k \mathbf{f}_{s,f}^t \right], \quad (40)$$

and the local London penetration depth

$$\lambda(\mathbf{r}) = \begin{cases} \lambda_f(r), & r < R_1, \quad r > R_2, \\ \lambda_s, & R_1 \leq r \leq R_2, \end{cases} \quad (41)$$

depends on the radius  $r$  and can be expressed via the amplitudes  $F(r)$  and  $P(r)$  as follows:

$$\lambda_{s,f}^{-2}(r) = \frac{8\pi^2 T_L}{\hbar c^2} \sum_{\omega_n} \sigma_{s,f} [Re[F_{s,f}^2(r)] - P_{s,f}^2(r)], \quad (42)$$

where  $F_s = F_L(\omega_n)$ ,  $P_s = P_L(\omega_n)$ ,  $F_f(r) = F_{f1}(r)$  ( $F_{f2}(r)$ ) and  $P_f(r) = P_{f1}(r)$  ( $P_{f2}(r)$ ) for  $r \leq R_1$  ( $r \geq R_2$ ), respectively. If triplet superconducting correlations dominate in a ferromagnetic region, the corresponding value of  $\lambda_f^{-2}(r)$  becomes negative, and the local screening current (40) is paramagnetic. At the same

time,  $\lambda_s^{-2}(r) > 0$  in the thin S shell and  $\lambda_f^{-2}(r) > 0$  in ferromagnetic layers  $\sim \xi_f$  near the S/F boundaries, where the direction of the screening current corresponds to the conventional diamagnetic Meissner effect. A superconducting state remains stable in the whole as long as the London penetration depth (42) averaged over the cross section of the S/F structure

$$\Lambda^{-2} = \frac{2\pi}{S} \int_0^{R_\infty} \frac{r dr}{\lambda^2(r)}, \quad S = \pi R_\infty^2 \quad (43)$$

is negative<sup>43</sup>. The external radius of the structure  $R_\infty$  is assumed to be large enough ( $R_\infty \gg \xi_n$ ) to neglect the effect of the external boundary on the solutions (23),(24). Substituting the solutions of the linearized Usadel equations (33),(34),(37),(38) into (42), we obtain the following expression for the effective magnetic penetration depth  $\Lambda_L$  of the orbital mode  $L$  that the temperature  $T$  is close to the critical temperature  $T_L$ :

$$\Lambda_L^{-2} = \Lambda_T^{-2} \sum_{\omega_n} \left\{ \text{Re} \left[ \bar{F}_L^2(\omega_n) \left( \frac{w}{R_1} + \frac{\sigma_f}{\sigma_s} C_L(k_n) \right) \right] - \bar{P}_L^2(\omega_n) \left( \frac{w}{R_1} + \frac{\sigma_f}{\sigma_s} C_L(q_n) \right) \right\}, \quad (44)$$

$$\Lambda_T^{-2} = \frac{16\pi^3 T \sigma_s R_1^2}{\hbar c^2 S}, \quad C_L(q) = \frac{R_2^2 K_{L-1}(qR_2) K_{L+1}(qR_2)}{R_1^2 2 K_L^2(qR_2)} - \frac{I_{L-1}(qR_1) I_{L+1}(qR_1)}{2 I_L^2(qR_1)} - \frac{w}{R_1}.$$

In the case of a second-order phase transition at  $T = T_L$  from the superconducting to the normal state, the order parameter  $\Delta_L$  disappears ( $\Delta_L, \bar{F}_s, \bar{P}_s \rightarrow 0$ ), and effective penetration depth (44) diverges ( $\Lambda_L \rightarrow \infty$ ). At  $T < T_L$ , the structure of the superconducting order parameter corresponding to the free energy minimum may differ from (7), and the equilibrium value of  $\Delta_L$  in the S/F cylinder must be determined with the help of complete nonlinear Usadel equations without using the linear approximation (3),(4). Therefore, expression (44) establishes only the relation between superconducting order parameter  $\Delta_L$  and the effective magnetic field penetration depth  $\Lambda_L$  in the S/F structure for  $L$  orbital mode at a temperature  $T$  close to superconducting transition temperature  $T_L$ .

Figure 5 shows the typical dependence of the effective penetration depth  $\Lambda$  on  $R_1$  for different values of  $\delta$ . One can easily see that switching between different orbital modes  $L \rightleftharpoons L+1$  (see Fig. 3) are accompanied by jumps in  $\Lambda/\Lambda_T$  due to qualitative changes in the radial structure and symmetry of the pair wave-functions and the singlet/triplet correlations distributions in the S/F structure<sup>71</sup>. Such abrupt changes of screening proper-

ties of S/F cylinder due to orbital modes switchings look similar to the  $0 - \pi$  transition in S/F/S trilayer<sup>72-74</sup>. Negative values of  $\Lambda$  correspond to the total paramagnetic response of the hybrid structure. Here we neglect the possibility of LOFF modulation along the S/F cylinder axis assuming that the homogeneous in  $z$  state exists in the planar hybrid structure under consideration (see Fig. 1). The effect of an in-axis LOFF instability on screening properties of a thin-walled superconducting cylinder filled with a ferromagnetic metal was studied in<sup>71</sup>. In contrast to switching of orbital modes  $L \rightleftharpoons L+1$ , the appearance of LOFF modulation along the  $z$  axis is not accompanied by abrupt changes in the screening properties of the S/F cylinder and results in the restoration of the diamagnetic response of the hybrid structure. For layered S/F structures similar effect was first analyzed in<sup>43</sup>.

## V. LITTLE-PARKS OSCILLATIONS

Now we proceed with calculations of  $T_c$  on external magnetic field  $\mathbf{H}$  applied along  $z$  axis. Figures 6,7 show

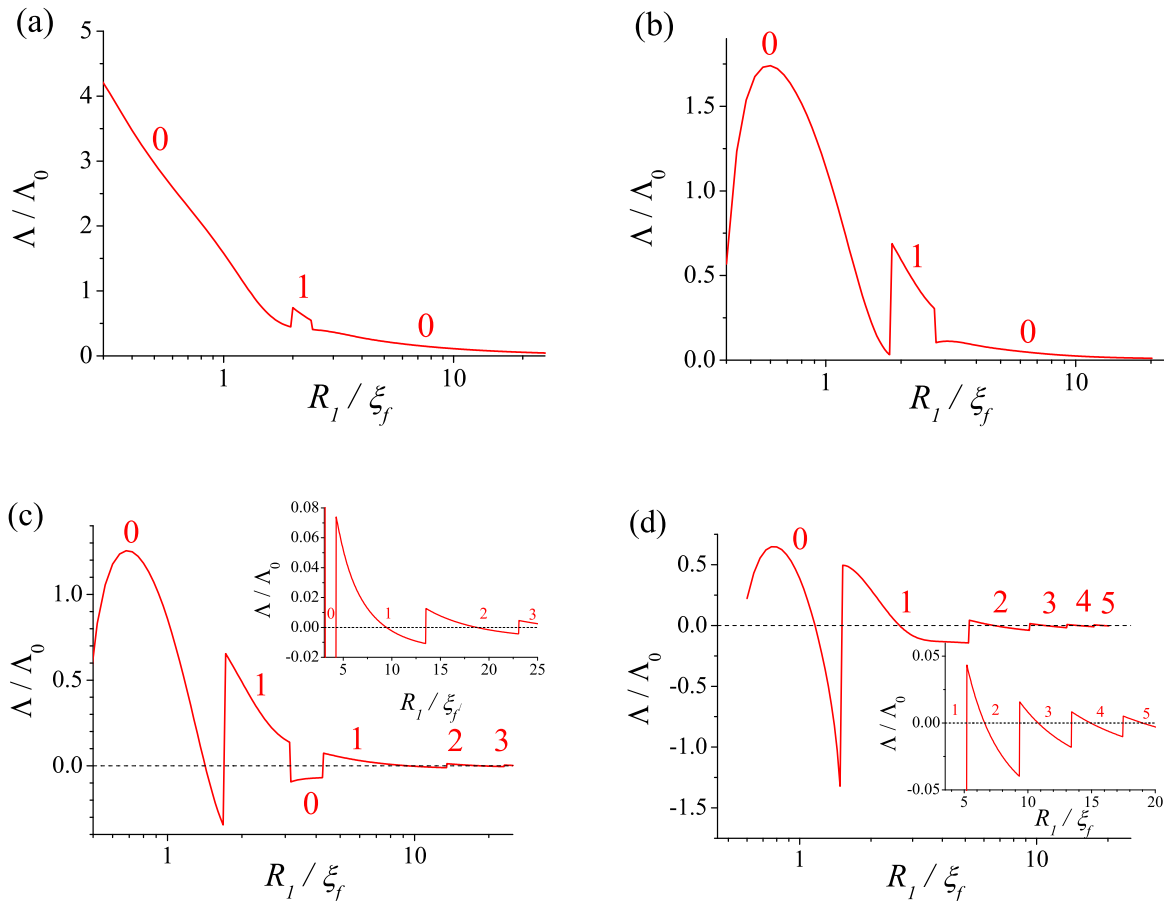


FIG. 5: (Color online) Typical dependences of the effective penetration depth  $\Lambda$  the internal radius  $R_1$  of the S ring in zero applied field ( $H = 0$ ) for different values of the parameters  $\delta$  characterizing a spin-activity of the S/F interface: (a)  $\delta = 0$ ; (b)  $\delta = 0.25$ ; (c)  $\delta = 0.3$ ; (d)  $\delta = 0.35$ . The numbers near the curves denote the corresponding values of vorticity  $L$ . The inserts show the zoom in the part of the curves in the rectangles. The other parameters are the same as in Fig. 3.

example of dependency of  $T_c$  on the external magnetic flux  $\phi_1 = \pi R_1^2 H / \Phi_0$  for different values of  $\delta$ . The phase boundary exhibits Little-Parks oscillations due to transitions between the states with different angular momenta  $L \rightleftharpoons L \pm 1$  of the superconducting order parameter. For  $R_1 \sim \xi_f$ , the  $T_c(H)$  phase boundary exhibits quasiperiodic oscillations versus  $H$  (Figure 6). One can observe a shift of the main  $T_c$  maximum toward nonzero  $H$ . The main maximum of  $T_c$  corresponds to the minima of both the orbital and exchange effects of superconductivity destruction. Since for chosen parameters of the S/F structure the exchange part of the depairing effect is minimal and the corresponding  $T_c$  is maximal for a state with a nonzero vorticity  $L$ , the orbital effect is cancelled at  $\phi_1 \approx L \neq 0$ . Thus, the main  $T_c$  maximum shifts to a certain nonzero  $\phi_1$  value<sup>53</sup>. Generation of long triplet correlations in F metal produces an additional depairing effect which results in a total decrease in the critical temperature  $T_c$  and a reduction of the interval of magnetic field in which magnetism and superconductivity coexist.

Figure 7 shows the LP quasiperiodic oscillations of  $T_c$  versus  $\phi_1$  for  $R_1 \gg \xi_f$  and for different values of  $\delta$ . One can observe a noticeable modification of the  $T_c(\phi_1)$  phase boundary when triplet superconducting correlations dominate in ferromagnetic regions (see panels (c) and (d) in Fig. 7) – the LP oscillations are destroyed for small values of the magnetic flux. To manifest this effect the inserts in Figure 7 show the dependence  $\Delta T_c(\phi_1) = T_c(\phi_1) - (c_1 \phi_1 + c_0)$  where the constants  $c_{0,1}$  are chosen to compensate monotonic growth of  $T_c$  with increasing of the magnetic flux. One can see that for  $\delta = 0.3$  and  $\delta = 0.35$  the curves  $\Delta T_c(\phi_1)$  show the Little-Parks oscillations if the magnetic flux  $\phi_1$  is large enough:  $\phi_1 \geq \phi_1^*$ , and the oscillations are destroyed for smaller values magnetic flux  $\phi_1$ . The value of cutoff parameter  $\phi_1^*$  grows with increasing the spin-active constant  $\delta$ .



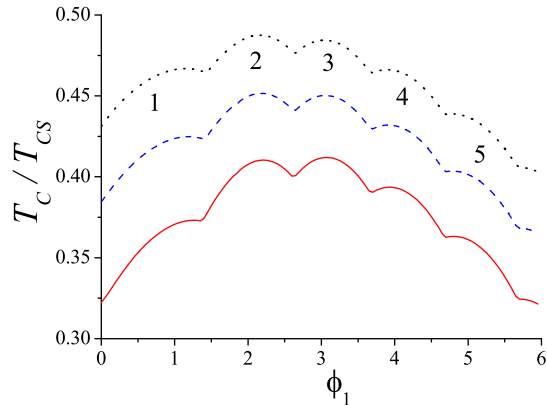


FIG. 6: (Color online) The dependences of the critical temperature  $T_c$  on the external magnetic field  $H$  for different values of the parameter  $\delta$  characterizing a spin-activity of the S/F interface:  $\delta = 0$  (dotted line);  $\delta = 0.25$  (dashed line);  $\delta = 0.35$  (solid line). The radius of the ring  $R_1 = 2.2\xi_f$ . The magnetic field  $H$  is measured in the units of the magnetic flux  $\phi_1$  enclosed in F core. The other parameters are the same as in Fig. 3.

## VI. SUMMARY

We have analyzed switching between superconducting states with different vorticities caused by the exchange field in multiply connected S/F hybrids associated with generation of odd-frequency spin-triplet correlations near S/F interface. As an example, we have considered mesoscopic thin-walled superconducting cylindrical shell embedded in ferromagnetic metal. A good electrical contact and the spin-active S/F interface between the S and F metals are assumed to assure a rather strong long ranged proximity effect. We suggest a mechanism of switching between superconducting states with different vorticities caused by prevalence of spin-triplet pairs in a consider-

able part of the S/F structure. The spin-active interface favors the emergence of the states with high vorticity  $L > 1$ . The screening properties of the mesoscopic S/F structure with a multiply connected geometry have been analyzed. The presence of spin-triplet superconducting correlations results in suppression of a diamagnetic response so that the effective magnetic field penetration depth  $\Lambda^{-2}$  can take a negative value indicating a paramagnetic Meissner effect. The observation of a paramagnetic response in the S/F setup of Fig. 1(a) would provide clear evidence the long-ranged odd-frequency triplet correlations. The behavior of the Little–Parks oscillations of the critical temperature  $T_c$  on an external magnetic flux  $\phi_1$  threading the ring was analyzed. The interplay between the orbital and exchange effects results in breaking of the periodicity of  $T_c(\phi_1)$  dependence and a slow modulation of the amplitude of the quasiperiodic oscillations. The Little–Parks oscillations are shown to be destroyed in the region of small values of the magnetic flux threading the ring if a spin-activity of S/F interface is strong enough so that the spin-triplet pairs prevail in the multiply connected hybrid.

## Acknowledgments

This work was supported by the Russian Science Foundation under the Grant No.15-12-10020 (A.V.S.), and the French ANR project SUPERTRONICS and OPTOFLUXONICS (A.I.B.). A.V.S. appreciate warm hospitality of the University Bordeaux, extended to him during the visits when this work was done. J.W.A.R. acknowledges funding from the EPSRC through an International Network Grant and Programme Grant (No. EP/P026311/1 and No. EP/N017242/1). J.W.A.R. also acknowledges funding from the Royal Society through a University Research Fellowship and with A.I.B., funding from the Leverhulme Trust and EU Network COST CA16218 (NANOCOBYBRI).

<sup>1</sup> A.I. Buzdin, Rev. Mod. Phys. **77**, 935 (2005).

<sup>2</sup> Yu.A. Izyumov, Yu.N. Proshin, M. G. Khusainov, Usp. Fiz. Nauk **172**, 113 (2002) [Sov. Phys. Usp. **45**, 109 (2002)].

<sup>3</sup> F.S. Bergeret, A.F. Volkov, K.B. Efetov, Rev. Mod. Phys. **77**, 1321 (2005).

<sup>4</sup> M. G. Blamire, J. W. A. Robinson, J. of Phys.-Cond. Matt. **26**, 453201 (2014).

<sup>5</sup> J. Linder and J.W.A. Robinson, Nature Physics **11**, 307 (2015).

<sup>6</sup> M. Eschrig, Rep. Prog. Phys. **78**, 10450 (2015).

<sup>7</sup> M. Giroud, H. Courtois, K. Hasselbach, D. Mailly, B. Panetier, Phys. Rev. B **58**, R11872 (1998).

<sup>8</sup> I. Sosnin, H. Cho, V.T. Petrashov, A.F. Volkov, Phys. Rev. Lett. **96**, 157002 (2006).

<sup>9</sup> R.S. Keizer, S.T.B. Goennenwein, T.M. Klapwijk, G. Miao, G. Xiao, A. Gupta, Nature **439**, 825 (2006).

<sup>10</sup> J. Wang, M. Singh, M. Tian, et al., Nature Physics **6**, 389 (2010).

<sup>11</sup> J. W. A. Robinson, J. D. S. Witt and M. G. Blamire, Science **329**, 59 (2010).

<sup>12</sup> J. W. A. Robinson, G. B. Halasz, A. I. Buzdin, and M. G. Blamire, Phys. Rev. Lett. **104**, 207001 (2010).

<sup>13</sup> T. S. Khaire, M. A. Khasawneh, and W. P. Pratt, Jr., N. O. Birge, Phys. Rev. Lett. **104**, 137002 (2010).

<sup>14</sup> C. Klose, T. S. Khaire, Y. Wang, et al., Phys. Rev. Lett. **108**, 127002 (2012).

<sup>15</sup> V.L. Berezinskii, JETP Lett. **20**, 287 (1974) [Pis'ma Zh. Eksp. Teor. Fiz. **20** 628 (1974) (in Russian)]

<sup>16</sup> F.S. Bergeret, A.F. Volkov, K.B. Efetov, Phys. Rev. Lett., **86**, 4096 (2001).

<sup>17</sup> A. Kadigrobov, R.I. Shekhter, M. Jonson, Europhys. Lett., **54**, 394 (2001).

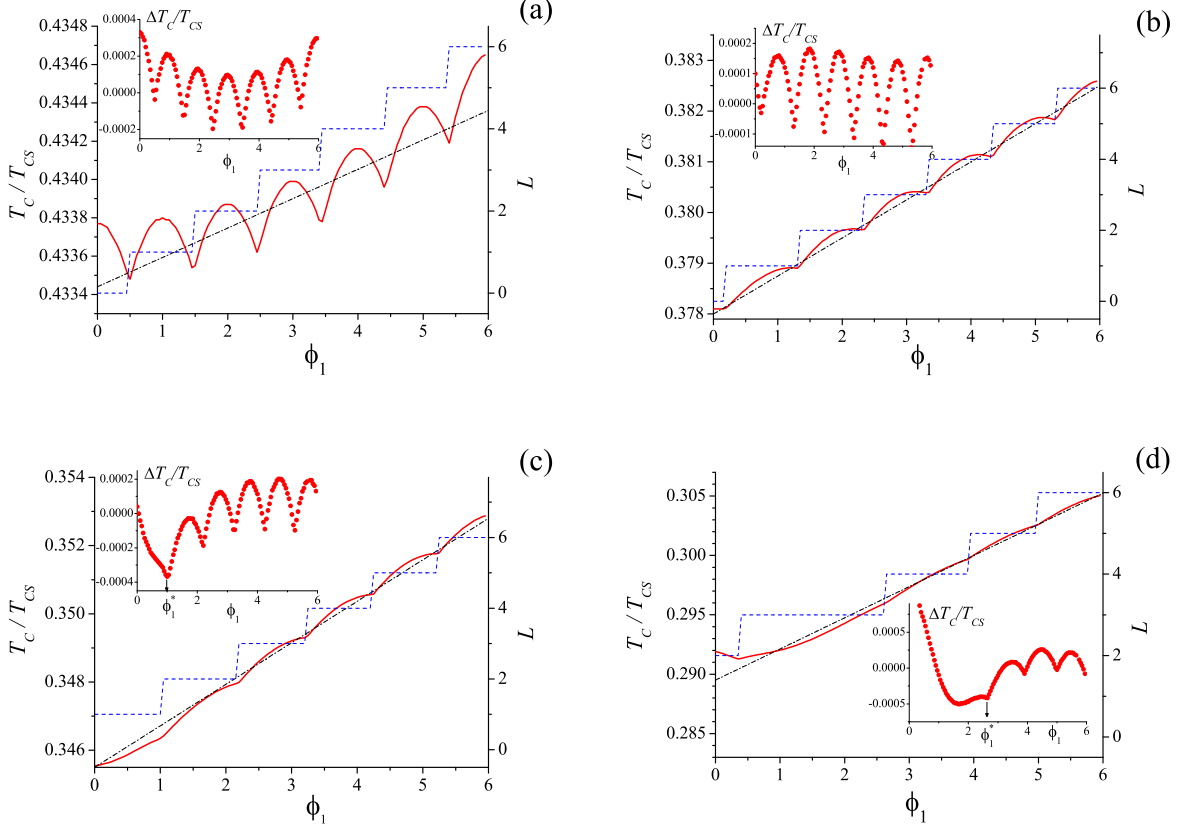


FIG. 7: (Color online) The dependences of the critical temperature  $T_c$  (solid line) and the vorticity  $L$  (dashed line) on the external magnetic field  $H$  for different values of the parameter  $\delta$  characterizing the spin-activity of the S/F interface: (a) –  $\delta = 0$ ; (b) –  $\delta = 0.25$ ; (c) –  $\delta = 0.3$ ; (d) –  $\delta = 0.35$ . The inserts show the dependence  $\Delta T_c(\phi_1) = T_c(\phi_1) - (c_1\phi_1 + c_0)$  (the functions  $c_1\phi_1 + c_0$  are shown by the dash-dotted line). The internal radius of the ring  $R_1 = 10\xi_f$ . The magnetic field  $H$  is measured in the units of the magnetic flux  $\phi_f$  enclosed in F core. The other parameters are the same as in Fig. 3.

- <sup>18</sup> M. Kompaniets, O. V. Dobrovolskiy, C. Neetzel, F. Porrati, J. Brotz, W. Ensinger, and M. Huth, *Appl. Phys. Lett.* **104**, 052603 (2014).
- <sup>19</sup> J. D. S. Witt, J. W. A. Robinson, and M. G. Blamire, *Phys. Rev. B* **85**, 184526 (2012).
- <sup>20</sup> J. W. A. Robinson, F. Chiodi, M. Egilmez, G. B. Halasz, M. G. Blamire, *Sci. Report* **2**, 699 (2012).
- <sup>21</sup> M. Egilmez, J. W. A. Robinson, J. L. MacManus-Driscoll, L. Chen, H. Wang and M. G. Blamire, *EPL* **106**, 37003 (2014).
- <sup>22</sup> J. W. A. Robinson, N. Banerjee, and M. G. Blamire, *Phys. Rev. B* **89**, 104505 (2014).
- <sup>23</sup> N. Banerjee, J. W. A. Robinson, M. G. Blamire, *Nature Communications* **5**, 4771 (2014).
- <sup>24</sup> P. V. Leksin, N. N. Garifyanov, I. A. Garifullin, Y. V. Fominov, J. Schumann, Y. Krupskaya, V. Kataev, O. G. Schmidt, B. Buchner, *Phys. Rev. Lett.* **109**, 057005 (2012).
- <sup>25</sup> X. L. Wang, A. DiBernardo, N. Banerjee, A. Wells, F. S. Bergeret, M. G. Blamire, J. W. A. Robinson, *Phys. Rev. B* **89**, 140508(R) (2014).
- <sup>26</sup> A. Singh, S. Voltan, K. Lahabi, and J. Aarts, *Phys. Rev. X* **5**, 021019 (2015).
- <sup>27</sup> Y. Gu, G.B. Halasz, J. W. A. Robinson, and M. G. Blamire, *Phys. Rev. Lett.* **115**, 067201 (2015).
- <sup>28</sup> A. Srivastava, *et al.*, *Phys. Rev. Appl.* **8**, 044008 (2017).
- <sup>29</sup> Y. Gu, *et al.*, *APL Materials* **2**, 046103 (2014).
- <sup>30</sup> P. SanGiorgio, S. Reymond, M. R. Beasley, J. H. Kwon, and K. Char, *Phys. Rev. Lett.* **100**, 237002 (2008);
- <sup>31</sup> I.T.M. Usman, K. A. Yates, J. D. Moore, *et al.*, *Phys. Rev. B* **83**, 144518 (2011).
- <sup>32</sup> K.M. Boden, W. P. Pratt, Jr., and N. O. Birge, *Phys. Rev. B* **84**, 020510(R) (2011).
- <sup>33</sup> Y. Kalcheim, O. Millo, M. Egilmez, J. W. A. Robinson, and M. G. Blamire, *Phys. Rev. B* **85**, 104504 (2012).
- <sup>34</sup> Y. Kalcheim, I. Felner, O. Millo, T. Kirzhner, G. Koren, A. Di Bernardo, M. Egilmez, M. G. Blamire, and J. W. A. Robinson, *Phys. Rev. B* **89**, 180506(R) (2014).
- <sup>35</sup> Y. Kalcheim, O. Millo, A. Di Bernardo, A. Pal, and J. W. A. Robinson, *Phys. Rev. B* **92**, 060501(R) (2015).
- <sup>36</sup> A. Di Bernardo, S. Diesch, Y. Gu, J. Linder, G. Divitini, C. Ducati, E. Scheer, M.G. Blamire, J.W.A. Robinson, *Nature Communications*, **6**, 9053 (2015).
- <sup>37</sup> K. A. Yates, L. A. B. Olde Olthof, M. E. Vickers, D. Prabhakaran, M. Egilmez, J. W. A. Robinson, and L. F. Cohen, *Phys. Rev. B* **95**, 094516 (2017).

- <sup>38</sup> K-R Jeon, C. Ciccarelli, A. J. Ferguson, H. Kurebayashi, L. F. Cohen, X. Montiel, M. Eschrig, J. W. A. Robinson and M. G. Blamire, *Nature Materials* **7**, 3411 (2017).
- <sup>39</sup> K. R. Jeon, C. Ciccarelli, H. Kurebayashi, L. F. Cohen, X. Montiel, M. Eschrig, S. Komori, J. W. A. Robinson, M. G. Blamire, *Phys. Rev. B* **99**, 024507 (2019).
- <sup>40</sup> M. Houzet, A. I. Buzdin, *Phys. Rev. B*, **76**, 060504(R) (2007)
- <sup>41</sup> F. S. Bergeret, A. F. Volkov, K. B. Efetov, *Phys. Rev. B*, **64**, 134506 (2001).
- <sup>42</sup> T. Yokoyama, Y. Tanaka, and N. Nagaosa, *Phys. Rev. Lett.*, **106**, 246601 (2011).
- <sup>43</sup> S. Mironov, A. Mel'nikov, A. Buzdin, *Phys. Rev. Lett.* **109**, 237002 (2012).
- <sup>44</sup> A. Di Bernardo, et al., *Phys. Rev. X* **5**, 041021 (2015);
- <sup>45</sup> A. V. Samokhvalov, A. S. Mel'nikov, A. I. Buzdin, *Phys. Rev. B*, **76**, 184519 (2007).
- <sup>46</sup> A. I. Buzdin, L. N. Bulaevskii, S. V. Panyukov, *Pis'ma Zh. Eksp. Teor. Fiz.* **35**, 147 (1982) [*JETP Lett.* **35** 178 (1982)].
- <sup>47</sup> A. I. Buzdin, M. Yu. Kupriyanov, *Pis'ma Zh. Eksp. Teor. Fiz.* **53**, 308 (1991) [*JETP Lett.* **53**, 321 (1991)].
- <sup>48</sup> A. I. Buzdin, B. Vujicic, M. Yu. Kupriyanov, *Zh. Eksp. Teor. Fiz.* **101**, 231 (1992) [*Sov. Phys. JETP* **74**, 124 (1992)].
- <sup>49</sup> V. L. Ginzburg, *Zh. Eksp. Teor. Fiz.* **31**, 202 (1956) [*Sov. Phys. JETP* **4**, 153 (1957)].
- <sup>50</sup> D. Saint-James, D. Sarma, E. J. Thomas, *Type-II Superconductivity*, Pergamon Press 1969.
- <sup>51</sup> W. A. Little, R. D. Parks, *Phys. Rev. Lett.*, **9**, 9 (1962).
- <sup>52</sup> W. A. Little, R. D. Parks, *Phys. Rev.*, **133**, A97 (1964).
- <sup>53</sup> A. V. Samokhvalov, A. S. Mel'nikov, J. P. Ader, A. I. Buzdin, *Phys. Rev. B*, **79**, 174502 (2009).
- <sup>54</sup> B. Krunavakarn, S. Yoksan, *Physica C*, **495**, 5 (2013).
- <sup>55</sup> B. Krunavakarn, *Physica C*, **527**, 63 (2016).
- <sup>56</sup> M. Alidoust, J. Linder, *Phys. Rev. B*, **82**, 224504 (2010).
- <sup>57</sup> R. P. Groff, R.D. Parks, *Phys. Rev.* **176**, 567 (1968).
- <sup>58</sup> S.V. Mironov, D.Yu. Vodolazov, Y. Yerin, A.V. Samokhvalov, A.S. Melnikov, and A. Buzdin, *Phys. Rev. Lett.* **121**, 077002 (2018).
- <sup>59</sup> O. Buisson, P. Gandit, R. Rammal, Y. Y. Wang, and B. Pannetier, *Phys. Lett. A* **150**, 36 (1990).
- <sup>60</sup> H.T. Jadallah, J. Rubinstein, P. Sternberg, *Phys. Rev. Lett.*, **82**, 2935 (1999).
- <sup>61</sup> V.N. Krivoruchko, E.A. Koshina, *Phys. Rev. B*, **66**, 014521 (2002).
- <sup>62</sup> F.S. Bergeret, A.F. Volkov, K.B. Efetov, *Phys. Rev. B*, **69**, 174504 (2004).
- <sup>63</sup> I.A. Garifullin, *Pis'ma Zh. Eksp. Teor. Fiz.* **93**, 674 (2011).
- <sup>64</sup> L. Usadel, *Phys. Rev. Lett.*, **25**, 507 (1970).
- <sup>65</sup> V.P. Mineev, K.V. Samokhin, *Introduction to Unconventional Superconductivity*, London: Gordon and Breach (1999).
- <sup>66</sup> T. Tokuyasu, J.A. Sauls, D. Rainer, *Phys. Rev. B*, **38**, 8823 (1988).
- <sup>67</sup> T. Champel, M. Eschrig, *Phys. Rev. B*, **71**, 220506(R) (2005).
- <sup>68</sup> M.Yu. Kupriyanov, V.F. Lukichev, *Sov. Phys. JETP* **67**, 1163 (1988).
- <sup>69</sup> S. Mironov, A. Buzdin, *Phys. Rev. B* **92**, 184506 (2015)
- <sup>70</sup> M. Abramowitz, I. A. Stegun, *Handbook of Mathematical Functions*, Natl. Bur. Stand. Appl. Math. Ser. No. 55 1965.
- <sup>71</sup> A.V. Samokhvalov, *JETP* **125**, 298 (2017).
- <sup>72</sup> N. Pompeo, K. Torokhtii, C. Cirillo, A. V. Samokhvalov, E. A. Ilyina, C. Attanasio, A. I. Buzdin, and E. Silva, *Phys. Rev. B*, **90**, 064510 (2014).
- <sup>73</sup> A.V. Samokhvalov, A.I. Buzdin, *Phys. Rev. B*, **92**, 054511 (2015).
- <sup>74</sup> M. J. Hinton, S. Steers, B. Peters, F. Y. Yang, and T. R. Lemberger, *Phys. Rev. B*, **94**, 014518 (2016).